PHILO

rsta.royalsocietypublishing.org

Research

Article submitted to journal

Subject Areas:
mathematical biology, applied mathematics, computational mathematics

Keywords:
neuron dynamics, self-pulsations, delay differential equations, bifurcation analysis

Author for correspondence:
Carlo R. Laing
e-mail: c.r.laing@massey.ac.nz

Theta neuron subject to delayed feedback: a prototypical model for self-sustained pulsing

Carlo R. Laing[1] and Bernd Krauskopf[2]

[1]School of Natural and Computational Sciences, Massey University, Private Bag 102-904, North Shore Mail Centre, Auckland 0745, New Zealand
[2]Department of Mathematics, The University of Auckland, Private Bag 92019, Auckland 1142, New Zealand

We consider a single theta neuron with delayed self-feedback in the form of a Dirac delta function in time. Because the dynamics of a theta neuron on its own can be solved explicitly — it is either excitable or shows self-pulsations — we are able to derive algebraic expressions for existence and stability of the periodic solutions that arise in the presence of feedback. These periodic solutions are characterized by one or more equally spaced pulses per delay interval, and there is an increasing amount of multistability with increasing delay time. We present a complete description of where these self-sustained oscillations can be found in parameter space; in particular, we derive explicit expressions for the loci of their saddle-node bifurcations. We conclude that the theta neuron with delayed self-feedback emerges as a prototypical model: it provides an analytical basis for understanding pulsating dynamics observed in other excitable systems subject to delayed self-coupling.

1. Introduction

The theta neuron model, or theta neuron for short, is a mathematical model designed to capture essential features of spiking or bursting neurons [1]. It takes the form of a differential equation for a single angular variable $\theta(t)$ 2 ($\pi; \pi]$

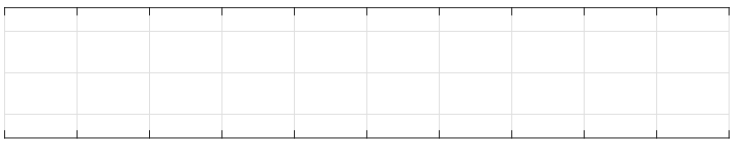

Figure 1. Coexisting stable periodic solutions of Eq. (1.1) for $\kappa = 1; \tau = 20$ and $I = -0{:}01$. Note that when θ reaches π from below it is reset to $-\pi$.

details of the excitability are not important when it comes to identifying underlying principles of self-sustained oscillations in the presence of delayed feedback. Figure 1 shows three periodic solutions of Eq. (1.1) that coexist and are characterized by one, two and three equidistant pulses being regenerated in the feedback loop over one delay interval. It is the existence and stability of these types of solutions that are the focus of this paper. The key technical property that we make use of here is that the dynamics of the theta neuron with delta-function self-feedback can be described equivalently by a discrete map for the spike times. Hence, periodic solutions of (1.1) correspond to periodic points under iteration, and their stability can be calculated explicitly by linearizing the map.

A number of other authors have studied oscillators with pulsatile interactions [18–20], exploiting the fact that it is often possible to explicitly calculate the effects of these interactions. One example is the leaky integrate-and-fire neuron [19], featuring a reset when the firing threshold is reached, which can be solved explicitly. However, that neuron model has the disadvantage of being phenomenological, whereas the theta neuron has been derived from a more complex Hodgkin-Huxley type model via the technique of phase reduction [1,2]. Note further that (1.1) is exactly equivalent under the transformation $V = \tan(\theta/2)$ to the quadratic integrate-and-fire (QIF) neuron given by the equation

$$\frac{dV}{dt} = I + V^2 + \kappa \sum_{i:\,-\tau < t_i < 0} \delta(t - t_i - \tau) \tag{1.2}$$

for the voltage V, along with the rule that if $V(t^-) = \infty$ then $V(t^+) = -\infty$ [21,22]. We will use this equivalence several times below to derive solutions of the theta neuron model.

We consider here two important subcases of Eq. (1.1): the case of $I < 0$ when the theta neuron is excitable and has positive (excitatory) self-coupling for $\kappa > 0$; for h122 0 Td e3sn 14.3f64 Tf 15.481 6 Td [(0)]TJ/F1

self-coupling. For ease of notation we define the input current I separately as

$$I = \begin{cases} I_m^2 & I < 0 \\ I_p^2 & I > 0 \end{cases} \tag{1.3}$$

for these two cases. In Sec. 2 we consider the case of $I_m^2 = I < 0$ and $\kappa > 0$ of the excitable theta neuron with excitatory self-feedback; we derive the existence of periodic orbits, determine their stability analytically, and give an explicit expression for the saddle-node bifurcations of these orbits. Section 3 concerns the case $I_p^2 = I > 0$ of a theta neuron firing periodically even without any feedback. We derive existence and stability of periodic orbits for $\kappa > 0$ and then show that these are related to those for $\kappa < 0$ via a simple geometric transformation; again, curves of saddle-node bifurcations are given explicitly. In Sec. 4 we consider the theta neuron with a feedback term that is smooth, rather than a delta function. The resulting system needs to be studied numerically, and we find that for both $I < 0$ and $I > 0$ the dynamics for excitatory coupling with $\kappa > 0$ are qualitatively as those of (1.1). For $I > 0$ and $\kappa < 0$

past firing times are evenly spaced with time T between them, meaning that T is the period of oscillation. It follows that

$$\frac{\tau}{n+1} < T < \frac{\tau}{n}.$$

The time until the neuron feels the next delta function is $\tau - nT$, which is less than T. Since $\theta(0) = \pi$ we have from (2.3) that

$$\theta(\tau - nT) = 2\tan^{-1}\left[-I_m \coth\left[I_m(\tau - nT)\right]\right].$$

The delta function moves θ to the new value:

$$\theta(\tau - nT^{+}) = 2\tan^{-1}\left[\tan\left(\frac{\theta(\tau - nT^{-})}{2}\right) + \kappa\right]. \tag{2.4}$$

Assuming that $\tan[\theta(\tau - nT^{+})/2] > I_m$, i.e. we are above the upper fixed point, the phase θ continues to increase and the neuron fires after a further time Δ. Again using (2.3), this happens when

$$\pi = 2\tan^{-1}\left[-I_m \coth\left(I_m\Delta - \coth^{-1}\left[\frac{\tan\left(\frac{\theta(\tau - nT^{+})}{2}\right)}{I_m}\right]\right)\right],$$

or, equivalently, when

$$I_m\Delta - \coth^{-1}\left[\frac{\tan\left(\frac{\theta(\tau - nT^{+})}{2}\right)}{I_m}\right] = 0. \tag{2.5}$$

Substituting (2.4) into (2.5) we get

$$\Delta = \frac{1}{I_m}\coth^{-1}\left[\kappa/I_m - \coth\left[I_m(\tau - nT)\right]\right].$$

We know that the amount of time the neuron waits before the delta function acts, $(\tau - nT)$ plus Δ, has to equal T, i.e. $\Delta + \tau - nT = T$. Thus we have $\Delta = (n+1)T - \tau$ and finally

$$(n+1)T = \tau + \frac{1}{I_m}\coth^{-1}\left[\frac{\kappa}{I_m} - \coth\left[I_m(\tau - nT)\right]\right]. \tag{2.6}$$

Recall that this expression is valid only for $\frac{\tau}{n+1} < T < \frac{\tau}{n}$. For $n = 0$ (2.6) gives the period T explicitly in terms of the other parameters. The periodic solutions shown in Fig. 1 with one up to three equidistant spikes per delay interval of length $\tau = 20$ in panels (a), (b) and (c) correspond to $n = 0, 1$ and 2, respectively.

Note from (2.5) was 8.9664 Tf 12.215 0 .04321 Td [(The) -2501([)]TJ/

nT3 2.6) that (...) 0.242 000

$\lambda = 1$. So if $\gamma \in f0; 1g$ then $\lambda = 1$ is the only root of g with magnitude 1. The case $\gamma = 0$ is ruled out and the case $\gamma = 1$ is covered by (ii).

(iv) Differentiating $g(\lambda) = 0$ with respect to γ we have

$$(n+1)\lambda^n \frac{d\lambda}{d\gamma} \quad \lambda^n + \gamma n \lambda^{n-1} \frac{d\lambda}{d\gamma} + 1 = 0$$

$$) \quad \frac{d\lambda}{d\gamma} = \frac{\lambda^n - 1}{\lambda^{n-1}[\lambda(n+1) - \gamma n]}. \tag{2.15}$$

Now if $\gamma \neq (n+1)/n$ (i.e. away from this instability), we have $\frac{d\lambda}{d\gamma}|_{\lambda=1} = 0$, reflecting that the root $\lambda = 1$ of g is always present. However, if $\gamma = (n+1)/n$ we have

$$\frac{d\lambda}{d\gamma} = \frac{\lambda^n \quad 1}{(n+1)(\lambda^n \quad \lambda^{n-1})};$$

which is undefined at $\lambda = 1$. With L'Hopital's rule we have

$$\lim_{\lambda \to 1} \frac{d\lambda}{d\gamma} = \lim_{\lambda \to 1} \frac{n\lambda^{n-1}}{(n+1)[n\lambda^{n-1} \quad (n \quad 1)\lambda^{n-2}]} = \frac{n}{n+1} > 0.$$

This is the speed at which the root leaves the unit circle.

(v) The only instability occurs when $h(1) = 0$, i.e. when $\gamma = (n+1)/n$. When $\gamma = 1$ the orbit is stable, so it must be stable for $0 < \gamma < (n+1)/n$.

(vi) For superstability we have $\gamma = 1$, which (from the definition of γ in (2.10)) implies that

$$\kappa = 2\coth(\tau \quad nT). \tag{2.16}$$

The equation for the existence of a periodic orbit is (2.7), and differentiating it with respect to τ we get

$$\operatorname{csch}^2[(n+1)T \quad \tau] \quad (n+1)\frac{dT}{d\tau} \quad 1 = \operatorname{csch}^2(nT \quad \tau) \quad n\frac{dT}{d\tau} \quad 1 \quad . \tag{2.17}$$

By using the identity $\operatorname{csch}^2 x = \coth^2 x \quad 1$ and substituting (2.7) into (2.17), then

Figure 2. Roots in the complex plane (with the unit circle shown) of the function $g(\lambda)$ from (2.12) for $n = 4$ as its parameter γ (represented by the colour bar) is varied for $0 \leq \gamma < 1$

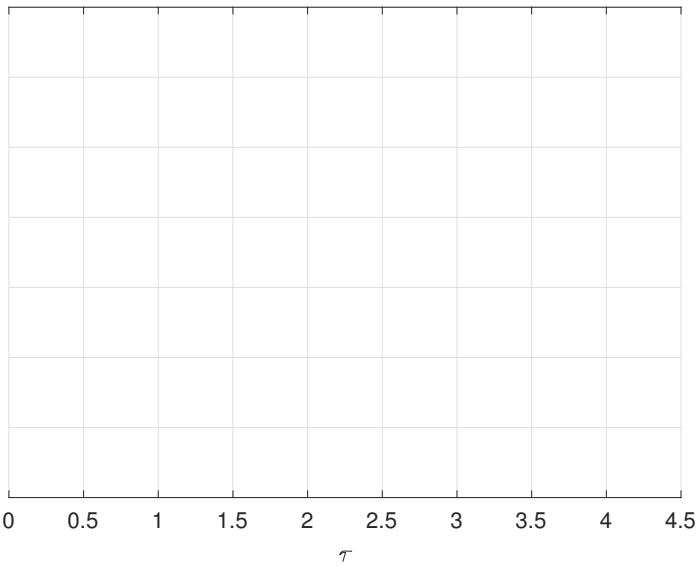

Figure 3. Branches of periodic solutions for $n = 0; 1; 2; 3; 4$ (see legend) of (1.1) with negative current I, shown by their period T as a function of the delay τ. Periodic solutions are stable along solid curves, unstable along dashed curves, and superstable at the minima of T; stars indicate saddle-node bifurcations. Here, $I = -I_m^2 = -1$ and $\kappa = 5$.

For $\kappa = 5$ we obtain the solution $\tau = \coth^{-1}(\kappa \quad 1) \quad 0{:}25541$, which is the position of the vertical asymptote in Fig. 3. The minimum in T of this curve for $n = 0$ occurs at $(\tau; T) = (\overline{}$

Figure 4. The Floquet multipliers of the different stable periodic solutions with $n = 0; 1; 2; 3; 4$ (see legend) for $\tau = 4$ in Fig. 3, as computed from (2.12). Here, $I = -I_m^2 = -1$ and $\kappa = 5$. Compare with Fig. 2.

minimum at $(\tau; T) = (\overline{T}=2; \overline{T})$ on the primary branch. It follows that the minimum on the $n = 1$ branch is at $(\tau; T) = (3\overline{T}=2; \overline{T})$, on the $n = 2$ branch at $(\tau; T) = (5\overline{T}=2; \overline{T})$, and on the nth branch at $(\tau; T) = ((2n + 1)\overline{T}=2; \overline{T})$. Thus, we conclude that the minimum on the nth branch occurs at its (nontransverse) intersection point with the line $T = 2\tau=(2n + 1)$.

We conclude this section by considering the properties of the different stable periodic solutions in the region of multistability. Figure 4 shows the sets of Floquet multipliers for the stable solutions given by (2.7) with $n = 0; 1; 2; 3; 4$ at $\tau = 4$ in Fig. 3. As discussed in Sec. (b), these multipliers are roots of the polynomial $g(\lambda)$ from (2.12) and can, thus, easily be found numerically for any value of γ (see (2.10)) which in turn depends on κ and τ. For solutions such as those in Fig. 3, the parameter γ tends to zero from above as one moves along a stable branch away from the saddle-node bifurcation where it is created. According to Proposition 1(i), the respective Floquet multipliers approach the unit circle from within as $\gamma \to 0$, namely at roots of unity; see also Fig. 2. This explains why the multipliers for smaller n are closer to the unit circle, which is certainly the case for $n = 0; 1; 2; 3$ in Fig. 4, meaning that the stability of the corresponding periodic solutions is already quite weak. This analytical result for the theta neuron (1.1) with Dirac delta function is in agreement with, and may serve as an explanation for, the observation in other contexts [10,28] of only weakly stable solutions with n spikes or pulses in the delay interval, whose Floquet multipliers are near roots of unity.

(d) Bifurcation curves in the $(\tau; \kappa)$-plane for negative current

The bifurcation of the branches in Fig. 3 can be continued in the additional parameter κ. Figure 5 shows in the (

Figure 5. Bifurcation curves in the $(\tau; \kappa)$-plane for $n = 0; 1; 2; 3; 4; 5; 6$ (see legend) of (1.1) with negative current I; compare with Fig. 3. The curve for $n = 0$ (black) is the locus of homoclinic bifurcation of the primary branch; no periodic solutions exist below and to the left of this curve. The curves for $n = 1; 2; 3; 4; 5; 6$ are the saddle-node bifurcations of the secondary branches. Here, $I = -I_m^2 = -1$.

$$(\tau_0^{(1)}; T^{(1)})$$

$$(\tau_0^{(2)}; T^{(2)})$$

$$(\overline{T}=2; \overline{T})$$

Figure 6. The points $(\tau_0^{(n)}; T^{(n)})$ (red crosses) on the primary branch of periodic solutions (blue curve) converge to its minimum at $(\tau; T) = (\overline{T}=2; \overline{T})$; these points map to the points of saddle-node bifurcation on the nth branch at $(\tau_0^{(n)} + nT^{(n)}; T^{(n)})$; compare with Fig. 3. Here, $I = -I_m^2 = -1$ and $\kappa = 5$.

where we have taken the physically meaningful of the two possible solutions. Substit1itgg (

In Fig. 6 the first 100 of the points $T^{(n)}$ for $\kappa = 5$ in (2.24) are plotted on the primary branch. This illustrates that $T^{(n)}$ converges to the value $\overline{T}$ at the minimum of the primary branch. Indeed,

$$\lim_{n \to \infty} \kappa(1+n) \qquad \sqrt{1+\kappa^2(n^2+n)} = \kappa/2$$

and

$$\lim_{n \to \infty} T^{(n)} = 2\coth^{-1}(\kappa/2) = \overline{T}.$$

The value of τ at which the saddle-node bifurcation of the nth branch occurs is $\tau^{(n)} = \tau_0^{(n)} + nT^{(n)}$; this expression depends on κ and the curves in Fig. 5 were obtained by plotting $\tau^{(n)}$ as a function of κ for various n s indicated.

3. Oscillating theta neuron for positive current

We now consider (1.1) with a positive current $I = I_p^2 > 0$, which means that the uncoupled theta

We1.1

As before, we can rescale either I_p; κ or τ to be 1, so set $I_p = 1$ and rewrite (3.2) as

$$(n+1)T = \tau + \frac{\pi}{2} - \tan^{-1}\left[\kappa + \tan\left(\tau - nT + \frac{\pi}{2}\right)\right]. \tag{3.3}$$

This is the equation relating the period T to the other parameters τ and κ, for a given integer n. As above, for $n = 0$ expression (3.3) gives T explicitly as

$$T(\tau) = \tau + \frac{\pi}{2} - \tan^{-1}\left[\kappa + \tan\left(\tau + \frac{\pi}{2}\right)\right] = \tau + \frac{\pi}{2} - \tan^{-1}[\kappa - \cot\tau]; \tag{3.4}$$

which is valid for $0 < \tau < \pi$. Note that, when $I = I_p = 1$, $d\theta/dt = 2$ except at the times at which the feedback acts, which simplifies the derivations below.

(b) Stability of periodic solutions for positive current

Determining the stability for $I = I_p^2 > 0$ is also similar to the excitable case. Assume again that the neuron has just fired at time t_0 and there are n past firing times in $(-\tau; 0)$. We wait $\tau - (t_0 - t_{-n})$ until the delta function acts, which maps θ from

$$\theta(\tau - t_0 + t_{-n}^-) = \pi + 2(\tau - t_0 + t_{-n})$$

to

$$\theta(\tau - t_0 + t_{-n}^+) = 2\tan^{-1}\left[\tan\left(\frac{\theta(\tau - t_0 + t_{-n}^-)}{2}\right) + \kappa\right].$$

We then wait a time Δ until the neuron fires at time t_1, where

$$\pi = 2\Delta + \theta(\tau - t_0 + t_{-n}^+).$$

Thus

$$t_1 = t_0 + (\tau - t_0 + t_{-n}) + \Delta = \tau + t_{-n} + \frac{\pi}{2} - \tan^{-1}\left[\tan\left(\tau - t_0 + t_{-n} + \frac{\pi}{2}\right) + \kappa\right]$$

and, in general,

$$t_i = \tau + t_{i-n-1} + \frac{\pi}{2} - \tan^{-1}\left[\tan\left(\tau - t_{i-1} + t_{i-n-1} + \frac{\pi}{2}\right) + \kappa\right].$$

This is a map giving the next firing time, t_i, in terms of the previous ones, back to t_{i-n-1}. Perturbing the firing times defined by this equation as in Sec. 2(b), we obtain the same matrix J as in (2.11). However, now for a periodic orbit with period T we have

$$\gamma = \frac{\sec^2(\tau - nT + \frac{\pi}{2})}{1 + [\tan(\tau - nT + \frac{\pi}{2}) + \kappa]^2} = \frac{\csc^2(\tau - nT)}{1 + [\kappa - \cot(\tau - nT)]^2}; \tag{3.5}$$

which is clearly positive for any value of κ.

(c) Branches of periodic orbits for positive current

As in Sec. 2(c), the primary branch of periodic solutions is given by (3.4

Figure 7. Branches of periodic solutions for $n = 0; 1; 2; 3; 4; 5$ of (1.1) with positive current I and positive κ, showing their period T as a function of the delay τ. Periodic solutions are stable along solid curves, unstable along dashed curves, and superstable at the minima of T and at the maxima of T with $\tau > 0$; stars indicate saddle-node bifurcations. Here, $I = I_p^2 = 1$ and $\kappa = 2$.

in (1.1) the term $1 + \cos\theta$ is equal to zero, so the feedback can have no effect. The period of this free oscillation is $\pi/I_p = \pi$. For the chosen value of κ the primary branch is entirely stable. On the other hand, all secondary branches have two saddle-node bifurcations on them, with an unstable middle sub-branch. Notice also that the secondary branches are increasingly tilted to the right as n increases, leading again to an increasing level of multistability with increasing τ.

A periodic orbit is superstable when $dT/d\tau = 0$, and this again occurs at the minima of the period but now also at the maximum period (with $\tau > 0$) where neighbouring branches meet. Differentiating $\dot{T} = 0$ when

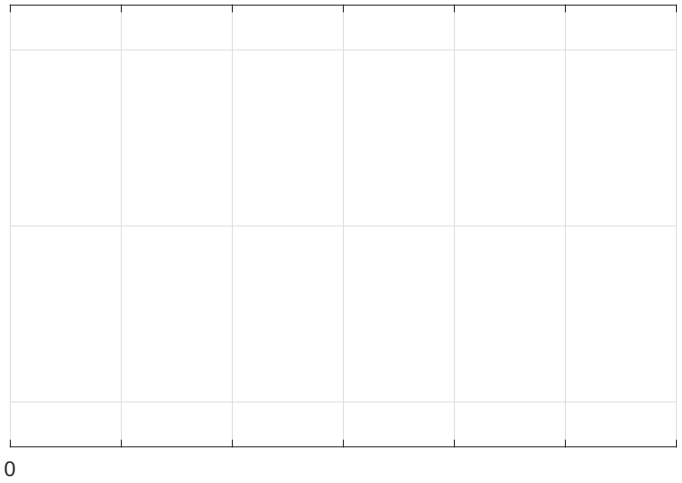

Figure 8. Branches of periodic solutions for $n = 0; 1; 2; 3; 4; 5$ of (1.1) with positive current I and negative κ, showing their period T as a function of the delay τ. Periodic solutions are stable along solid curves, unstable along dashed curves, and superstable at the minima of T; stars indicate saddle-node bifurcations. Here, $I = I_p^2 = 1$ and $\kappa = -2$; compare with Fig. 7.

For positive current $I = 1$ *and given* $n \quad 0$*, the* n*th branch of periodic orbits of* (3.3) *for* $\kappa = K > 0$ *maps to the* n*th branch for* $\kappa = \quad K < 0$ *under rotation over* π *about the point*

$$(\tau_c; T_c) \rightleftarrows ((

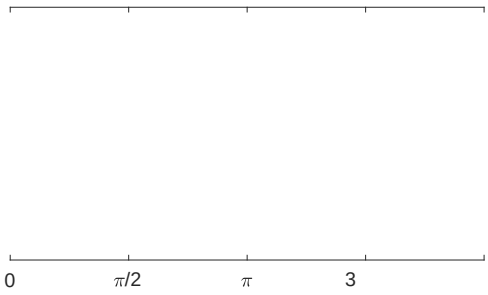

Figure 10. The pulsatile function $P(\theta)$ given in (4.2) as used in the theta neuron with smooth self-feedback (4.1).

to the possibility of multistability. The case of excitatory self-feedback is shown in the upper half of the (τ, κ)-plane where $\kappa > 0$. Notice that the respective cusp points, where the two curves defined by (3.10) come together, are minima here. Figure 9 also shows the curves of saddle-node bifurcations for $n = 1, 2, 3, 4, 5$ for the case of inhibitory coupling, namely in the lower half of the (τ, κ)-plane where $\kappa < 0$. These curves can be obtained from Eq. (3.10) (via (3.9)), now for negative

Figure 11. Coexisting stable periodic solutions of Eqs. (4.1)–(4.2) for $I = -1$, $\kappa = 2$ and $\tau = 4$. Note that when θ reaches π from below it is reset to $-\pi$. Compare with Fig. 1.

orbits must be expected to undergo standard bifurcations; see, for example, [39–42]. Periodic solutions of DDEs such as (4.1)–(4.2) are not known analytically but must be found with numerical methods [43,44]. To find (stable) periodic solutions we numerically integrate Eq. (4.1)–(4.2) with Matlab's dde23 integration routine. We then continue such periodic solutions in a parameter with the software DDE-BIFTOOL [31]. This allows us to compute branches of periodic solutions, regardless of whether they are stable or not, to identify their bifurcations, and to continue the respective bifurcation curves in a two-dimensional parameter space.

(a) Excitable smooth theta neuron

We again first consider the case of an excitable smooth theta neuron with $I < 0$, which means that we must have $\kappa > 0$ in (4.2) to obtain self-sustained solutions. Figure 11 shows typical coexisting >

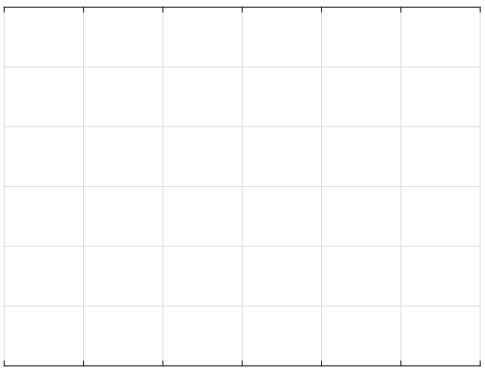

Figure 12. Branches of periodic solutions for $n = 0; 1; 2; 3$ (left to right) of Eqs. (4.1)–(4.2) with negative current I, found by numerical continuation and shown by their period T as a function of the delay τ. Periodic solutions are stable along solid curves and unstable along dashed curves; stars indicate saddle-node bifurcations. Here, $I = -1$ and $\kappa = 2$, and the three stable solutions in Fig. 11 are those at $\tau = 4$. Compare with Fig. 3.

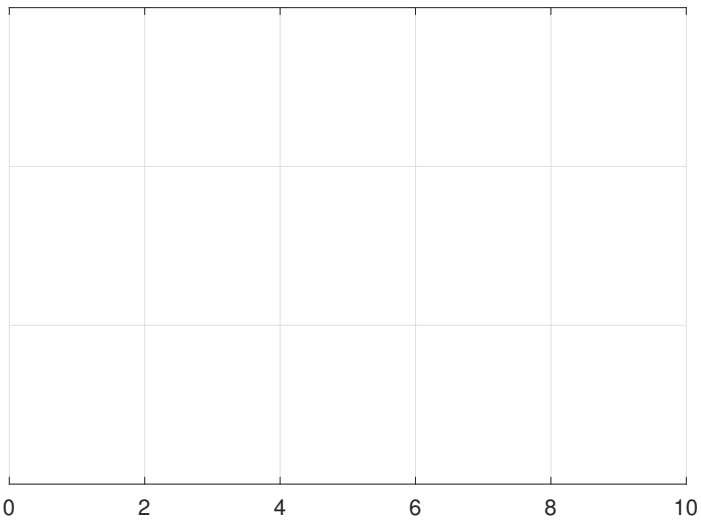

Figure 14. Periodic solutions of (4.1)-(4.2) with positive current I and positive κ, shown by period T as a function of the delay τ. This single branch was found by numerical continuation and has been split up at its maxima into segments associated with additional firing events $n = 0; 1; 2; 3; 4; 5$. Periodic solutions are stable along solid curves and unstable along dashed curves; stars indicate saddle-node bifurcations. Here, $I = 1$ and $\kappa = 1$. Compare with Fig. 7.

This is quite remarkable given that the feedback spike $P(\theta)$ in (4.2) is of a considerable width and not close to a Dirac delta function.

(b) Intrinsically oscillating smooth theta neuron

We now consider the smooth theta neuron (4.1)–(4.2) with positive I when, in the absence of coupling, the neuron fires periodically with period $\pi/\sqrt{I}$. When κ is positive the self-coupling is excitatory and numerical continuation started from a stable periodic solution results in the single branch of periodic solutions shown in Fig. 14. While the periodic solution varies smoothly along the branch, successive segments of it can still be associated with an increasing number of firings within a single delay period. We find that the transitions between consecutive numbers of firings

Figure 15. Saddle-node bifurcation curves in the $(\tau; \kappa)$-plane with $n = 1; 2; 3; 4; 5$ (see legend) of Eqs. (4.1)–(4.2) with positive current $I = 1$, found by numerical continuation from the respective saddle-node bifurcations in Fig. 14. Compare with Fig. 9 for $\kappa > 0$.

Figure 16.

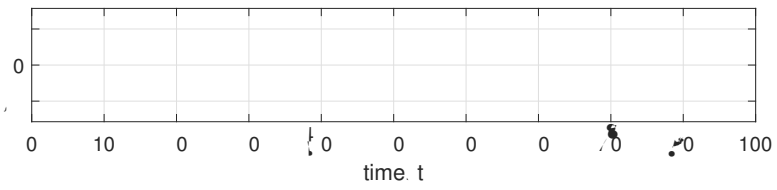

Figure 17. Solutions of (4.1)–(4.2) with $I = 1$ and $\kappa = -1$ for $\tau = 2.9$ (a), $\tau = 3.05$ (b) and $\tau = 3.3$ (c) illustrate period-doubling to chaotic spiking.

respectively. The statement that the solution in panel (c) is chaotic has been checked by verifying that it features a positive Lyapunov exponent.

Overall, we find a more diverse picture for the case that the theta neuron is intrinsically oscillating. For excitatory self-feedback there is still excellent agreement between the theta neuron (1.1) with Dirac delta function and the smooth theta neuron (4.1)–(4.2). For inhibitory self-coupling, on the other hand, we still find a single branch with pairs of saddle-node bifurcations as for system (1.1), but the smooth DDE (4.1)–(4.2) now features additional bifurcations that lead to more complicated dynamics in certain ranges of the delay τ, including chaotic spiking. It might be argued that this more complex behaviour results from the somewhat non-physical nature of

techniques) in different contexts as well [7,13]. To test the predictive power of our results for delta-function feedback, we investigated a single theta neuron with smooth delayed self-coupling. This

2. Ermentrout B. 1996 Type I membranes, phase resetting curves, and synchrony. *Neural Computation* **8**, 979–1001.
3. Murray JD. 1990 *Mathematical Biology*. Springer.
4. Izhikevich E. 2007

23. Ermentrout GB, Terman DH. 2010 *Mathematical Foundations of Neuroscience*. New York, NY: Springer.
24. Klinshov V, Lücken L, Shchapin D, Nekorkin V, Yanchuk S. 2015 Emergence and combinatorial accumulation of jittering regimes in spiking oscillators with delayed feedback. *Physical Review E* **92**, 042914.
25. Klinshov V, Lücken L, Shchapin D, Nekorkin V, Yanchuk S. 2015 Multistable jittering in oscillators with pulsatile delayed feedback. *Physical Review Letters* **114**, 178103.
26. Ruschel S, Krauskopf B, Broderick NG. 2020 The limits of sustained self-excitation and stable periodic pulse trains in the Yamada model with delayed optical feedback. *Chaos* **30**, 093101.
27. Yanchuk S, Perlikowski P. 2009 Delay and periodicity. *Physical Review E* **79**, 046221.
28. Terrien S, Pammi VA, Krauskopf B, Broderick NGR, Barbay S. 2021 Pulse-timing symmetry breaking in an excitable optical system with delay. *Physical Review E* **103**, 012210.
29. Kuznetsov Y. 2004 *Elements of Applied Bifurcation Theory*. Springer.
30. Doedel EJ, Oldeman BE. 2010 *AUTO-07p: Continuation and Bifurcation Software for Ordinary Differential Equations*. Department of Computer Science, Concordia University, Montreal, Canada. With major contributions from A. R. Champneys, F. Dercole, T. F. Fairgrieve, Y. Kuznetsov, R. C. Paffenroth, B. Sandstede, X. J. Wang and C. H. Zhang; available at http://www.cmvl.cs.concordia.ca/
31. Sieber J, Engelborghs K, Luzyanina T, Samaey G, Roose D. 2015 *DDE-BIFTOOL Manual — Bifurcation analysis of delay differential equations*. arXiv preprint arXiv:1406.7144; available at: https://sourceforge.net/projects/ddebiftool
32. Hashemi M, Valizadeh A, Azizi Y. 2012 Effect of duration of synaptic activity on spike rate of a Hodgkin-Huxley neuron with delayed feedback. *Physical Review E* **85**, 021917.
33. Laing CR. 2014 Derivation of a neural field model from a network of theta neurons. *Physical Review E* **90**, 010901.
34. Luke TB, Barreto E, So P. 2013 Complete classification of the macroscopic behavior of a heterogeneous network of theta neurons. *Neural Computation* **25**, 3207–3234.
35. Chandra S, Hathcock D, Crain K, Antonsen TM, Girvan M, Ott E. 2017 Modeling the network dynamics of pulse-coupled neurons. *Chaos* **27**, 033102.
36. Earl MG, Strogatz SH. 2003 Synchronization in oscillator networks with delayed coupling: A stability criterion. *Physical Review E* **67**, 036204.
37. Yeung MS, Strogatz SH. 1999 Time delay in the Kuramoto model of coupled oscillators. *Physical Review Letters* **82**, 648.
38. Lee W, Ott E, Antonsen T. 2009 Large coupled oscillator systems with heterogeneous interaction delays. *Physical Review Letters* **103**, 44101.
39. Diekmann O, van Gils S, Verduyn Lunel SM, Walther HO. 1995 *Delay Equations, Functional-, Complex-, and Nonlinear Analysis*. New York, NY: Springer.
40. Guo S, Wu J. 2013 *Bifurcation Theory of Functional Differential Equations*. Springer.
41. Hale JK, Verduyn Lunel SM. 1993 *Introduction to Functional Differential Equations*. New York, NY: Springer.
42. Smith H. 2011 *An Introduction to Delay Differential Equations with Applications to the Life Sciences*. Springer.
43. Krauskopf B, Sieber J. 2022 (to appear) Bifurcation analysis of systems with delays: methods and their use in applications.

In *Controlling Delayed Dynamics: Advances in Theory, Methods and Applications* (ed. D Breda), pp. 215–275. Springer.
44. Roose D, Szalai R. 2007 Continuation and bifurcation analysis of delay differential equations. In *Numerical continuation methods for dynamical systems*